Available online at www.sciencedirect.com
SCIENCE DIRECT®
Journal of Nuclear Materials 351 (2006) 133–140
journal of nuclear materials
www.elsevier.com/locate/jnucmat

Diffusion of He interstitials in grain boundaries in α-Fe

F. Gao *, H. Heinisch, R.J. Kurtz

Pacific Northwest National Laboratory, MS K8-93, P.O. Box 999, Richland, Washington 99352, USA

Abstract

Helium diffusion in metals is a complex process due to its very low solubility in solids and its ability to be trapped by vacancy type defects or impurities. The preferential positions and predominant migration mechanisms of He atoms depend on temperature, as well as the presence of other intrinsic or irradiation induced defects that can act as traps for He. This work presents results of a systematic molecular dynamics study of the diffusion mechanisms of He atoms in grain boundaries in α-Fe. Two grain boundaries, $\Sigma 11\langle 110\rangle\ \{323\}$ and $\Sigma 3\langle 110\rangle\ \{112\}$, were used for the current investigations. The low-temperature (about 0 K) equilibrium structures of these grain boundaries were determined using standard molecular dynamics relaxation techniques, with a flexible border condition. The migration of He atoms were followed for 1–14 ns, at temperatures between 600 and 1200 K. The diffusion coefficient of He atoms using the mean square displacements of He atoms, and the effective migration energies were determined. We found that He atoms diffuse rapidly in the Σ11 grain boundary, where the binding energy of a He atom to the boundary is high. He migration is primarily one-dimensional along specific directions, but a few directional changes were observed at higher temperatures. In the Σ3 grain boundary, where the He binding energy is low, He atoms migrate one-dimensionally at low temperature, two-dimensionally at intermediate temperature and three-dimensionally at higher temperature. The different activation energies and diffusion mechanisms in these two representative grain boundaries suggests that the atomic structures of the grain boundaries play an important role in the diffusivity of He.

1. Introduction

The high energy neutrons ($E > 1$ MeV) produced in nuclear fusion environments can interact strongly with the structural materials of a fusion device, causing a high rate of helium production by (n,α) reactions. The solubility of He in metals is extremely low, and this can produce significant changes in microstructure and mechanical properties, potentially embrittling the materials even at extremely low concentrations [1,2]. High helium concentrations can lead to the formation of helium bubbles that enhance void swelling due to large increases in the cavity density [3], and produce surface roughening and blistering [4]. At low temperatures He can lead to irradiation hardening [5] and fatigue life by acting as an obstacle to the movement of dislocations [6]. At high temperatures He can result in significant degradation of the tensile, creep and fatigue properties. These effects are caused by He bubbles in grain boundaries (GBs), which can initiate microcracks and result in premature failure under stress [7]. The extent of the degradation depends on the temperature, He concentration and production rate,

* Corresponding author. Tel.: +1 509 376 6275; fax: +1 509 376 5106.
E-mail address: fei.gao@pnl.gov (F. Gao).

0022-3115/$ - see front matter © 2006 Elsevier B.V. All rights reserved.
doi:10.1016/j.jnucmat.2006.02.015

stress, composition and microstructure of the materials. The formation of He bubbles both in bulk and GBs remains one of the most important issues in nuclear fusion technology. Interpretations of experimental information suggest that GBs provide fast diffusion paths for He atoms [8], and that He accumulation, both in the bulk and at GBs, has major consequences for structural integrity of first-wall materials. Thus, it is important to have a detailed knowledge of He diffusion in both bulk and GBs, that includes trapping and detrapping, the interaction of He with microstructures, the mobility of small helium–vacancy clusters, and the nucleation of helium bubbles. Computer simulations provide an important method to obtain insight and fundamental understanding of the complex atomic-level processes of defects controlling microstructural evolution in advanced ferritic steels. Particularly, molecular dynamics (MD) method has been widely employed to study the diffusion of defects and defect clusters in metals [9,10].

Recently, several computer simulations have been employed to yield important understanding of He behavior in bcc metals [11–13] and fcc metals [6,14]. Their results have shown that the binding energies of an interstitial helium atom, an isolated vacancy and a self-interstitial iron atom to a helium–vacancy cluster do not depend much on cluster size, but rather on the helium-to-vacancy ratio in α-Fe [11]. The binding energy of a vacancy to a helium–vacancy cluster increases as the ratio of He to vacancies increases, which suggests that helium increases cluster lifetime by dramatically reducing thermal vacancy emission. The binding energy of a helium atom or an iron atom to a helium–vacancy cluster decreases with increasing He/vacancy ratio, which indicates that thermal emission of self-interstitial atoms, as well as thermal helium emission, may take place from the cluster more easily at a higher helium-to-vacancy ratio. In order to understand the mechanisms responsible for the formation of He–vacancy clusters, the molecular dynamics (MD) method has been combined with kinetic Monte Carlo methods to study the migration and clustering of transmutant helium gas atoms in α-Fe, with particular emphasis on the high mobility of small vacancy–He clusters [12]. The results show that substitutional helium can jump into vacancies situated at both first and second nearest neighbor position in the bcc lattice, with relatively low activation barriers of 0.015 and 0.66 eV, respectively. The helium atoms are strongly bound to the He–vacancy clusters, with binding energy of ~2 eV, which leads to a very long thermal stability of the clusters. Atomistic calculations also demonstrate the strong binding of He to GBs [13] in α-Fe. Both substitutional and interstitial He atoms are trapped at GBs. Moreover, interstitial He is more strongly bound (~0.5–2.7 eV) to the GB core than substitutional He (~0.2–0.8 eV), and binding energy increases linearly with GB excess volume. Similar binding behavior of He atoms to GBs has been found in fcc nickel [14], and helium atoms placed in a symmetric tilt boundary cause the boundary to reconstruct, with He atoms more strongly bound to each other than in the bulk. These results suggest that GBs act as sinks to trap He atoms, and that they are possible sites for the nucleation of He bubbles, particularly at low temperature.

In modeling bubble nucleation at extended defects, such as dislocations and GBs, both the flux of He atoms to them from the bulk and the He diffusion along the extended defects must be considered. However, the diffusion constant for He diffusion along an extended defect is expected to depend significantly on the type of extended sink (dislocations or GBs). It has been demonstrated that the large variation in density and size of bubbles at different GBs observed in fcc Cu implanted with He at 738 K may be correlated with the varying atomistic structures of the GBs, which suggests that the GB's structure is important for the diffusivity of He along GBs [15]. As described in [10], we have initiated a systematic study to characterize the interaction of He with extended defects (dislocations and GBs) in a fusion relevant structural material such as ferritic steel. The grain boundary structures and the binding of He to GBs in α-Fe have been explored previously using computer simulations [13]. In this paper, the diffusion mechanisms of He atoms in grain boundaries will be studied using molecular dynamics (MD) methods, and the results will be compared with those obtained in bulk α-Fe.

2. Simulation methods

Most of the details of the methodology used in the calculations of the atomic arrangement of GBs have been described elsewhere [16,17]; thus, only the central principles are described in this paper. The model consists of a two part computational cell, rectangular in shape. The inner part, region I, contains movable atoms, while region II supplies

neighbors for region I, with a semi-rigid boundary condition. The equilibrium structures of GBs at 0 K are obtained via relaxation using molecular dynamics with an energy quench. The two grains are free to move and undergo displacements in all three directions, which occurs during relaxation via a viscous drag algorithm. Periodic boundary conditions are applied in the directions perpendicular to the normal direction of the GB plane. Two symmetric tilt GBs are employed to study He diffusion, all with a common $\langle 1\,0\,1\rangle$ tilt axis. The two GBs are $\Sigma 3\{1\,1\,2\}$ $\Theta = 70.53°$ and $\Sigma 11\{3\,2\,3\}$ $\Theta = 50.48°$. The shape of the MD block is rectangular with dimension 59.6 Å × 66.0 Å × 56.8 Å (18,816 atoms) and 57.5 Å × 66.0 Å × 56.8 Å (17978 atoms) for $\Sigma 3$ and $\Sigma 11$ GB, respectively.

The lowest energy configurations of a single He atom at the GBs were determined by raising the lattice temperature to 1000 K, with simulation time up to about 10 ps, and then slowly cooling down to 0 K. MD simulations of He diffusion were performed in the temperature range from 600 K to 1200 K, and the migration of He atoms were followed for 1–14 ns, which depends on temperature. The diffusivity of He atoms can be determined from the sum of the mean square displacements (MSD) of He atoms. For example, the diffusion coefficient of a He atom can be obtained by

$$D = \frac{\mathrm{MSD}}{6t}, \tag{1}$$

where $\mathrm{MSD} = \sum_{i=1}^{N} [\vec{r}_i(t) - \vec{r}_i(0)]^2$. This is accurate in the limit of large simulation time t. Therefore, the simulations were preformed over several tenths of nanoseconds. In the present simulations, considerable fluctuation in MSD is observed, particularly at low temperatures considered. To accurately calculate the diffusion coefficient of He atoms, the method used here is based on decomposing the single trajectory into a set of shorter independent segments with equal duration and applying Eq. (1) to each segment to calculate an average MSD, D_i (i indicates ith time interval for the segments). The time interval of segments is changed from 10 ps to 500 ps, which depends on the temperature, followed by averaging D_i over all time intervals. The similar treatment has been successfully applied to 1D and 3D diffusion of defect clusters in metals [9,10]. With the diffusion coefficients of He atoms obtained at different temperatures, the activation energy for He migration in GBs, E_m, can be estimated from the Arrhenius relation

$$D = D_0 \exp\left(-\frac{E_m}{k_\beta T}\right), \tag{2}$$

where D_0 is the pre-exponential factor and k_β is the Boltzmann constant.

The Fe–Fe interaction is described by the potential developed by Ackland et al. [18] based on the Finnis–Sinclair formalism, with a cut-off radius of 0.373 nm, between the second and third nearest neighbor shell. The cohesive energy for bcc Fe given by this potential is −4.42 eV/atom, and the lattice parameter is 0.28665 nm. The Fe–He potential was fit to ab initio calculations of small He–Fe clusters by Wilson and Johnson [19], with a cut-off distance of 0.38 nm. A classical potential developed by Beck [20] was used to describe He–He interaction, but it was refit to decrease the cut-off distance to 0.54857 nm to improve computational efficiency. With this change the cohesive energy of fcc He is −0.005678 eV/atom, as compared with the value of −0.00714 eV/atom given by the original potential. The formation energies of an interstitial He atom, a substitutional He atom, a vacancy and a self-interstitial atom were calculated to be 5.25, 3.25, 1.70 and 4.88 eV, respectively. These values are consistent with those reported previously [11].

3. Grain boundary structures and He binding properties

First the γ surfaces were calculated to explore the minimum energy structures of the GBs by constructing a series of atomic configurations in which the grains were translated relative to one another, as detailed in [13]. The cell of non-identical displacements, which defines the set of unique in-plane translations, was divided into a grid of points, and then the displacement-shift-complete (DSC) lattice was used as the basis of the grid. The GB energy was calculated at each point on the grid using a partial relaxation approach that includes local atomic displacements and rigid translations of the grains normal to the GB plane, but not parallel to it. Local minima on the γ surface correspond to relative translations of the grains producing stable or metastable GB structures. Such structures were individually examined by full relaxation. The deepest energy minimum corresponds to the ground state structure of the GB. Fig. 1(a) and (b) show the calculated ground state structures for the $\Sigma 3\{1\,1\,2\}$ and $\Sigma 11\{3\,2\,3\}$ GBs, respectively, where dark and light spheres denote atom positions in

alternating {1 1 0} planes perpendicular to the ⟨1 1 0⟩ tilt axis. The upper and lower grains are not distinguished by different symbols. The GB energy per unit area, γ_{gb}, can be determined by integrating the energy distribution function over several repeat periods. The values of γ_{gb} for the $\Sigma3\langle110\rangle\{112\}$ and $\Sigma11\langle110\rangle$ {3 2 3} GBs are 0.3 and 1.0 J/m^2, respectively. To our knowledge, there are no experimental values of GB energies to compare with the current results. However, it should be noted that the calculated free surface energies using the potential employed are slightly low relative to experimentally measured values in α-Fe, which are typically in the neighborhood of 1.6–2.3 J/m^2. It is most likely that the present calculations may give slightly low values of GB energies, although the potential employed provides a good description of the structural properties of bcc Fe.

Binding of He atoms to GBs was studied by insertion of a single He atom in either a substitutional or interstitial location, and then relaxing the simulation block using MD method with an energy quench. Because of the large variation of excess volume in the GB core, a large number of different starting positions for the He atom were examined. Binding energies at a particular site α of either substitutional or interstitial He in and near the GB core, E_B^α, were obtained from the equation

$$E_B^\alpha = E_{gb}^\alpha - E_{gb} - E_f^\alpha, \tag{3}$$

where E_{gb}^α is the GB energy with a He atom at site α, E_{gb} is the GB energy without a He atom, and E_f^α is the formation energy of a He atom at site α in bulk Fe. The maximum binding energy of a substitutional or interstitial He to the GB is plotted as a function of GB energy in Fig. 2. It can be seen that there is an excellent correlation between the maximum binding energy for both substitutional and interstitial He and the GB energy, i.e., the maximum binding energy generally increases with increasing GB energy. The strong binding of interstitial He to the GB, relative to the bulk, is similar to the findings obtained by Baskes and Vitek for He in Ni [14]. The various binding energies in the different GBs will affect the diffusion and migration mechanisms of He atoms in α-Fe.

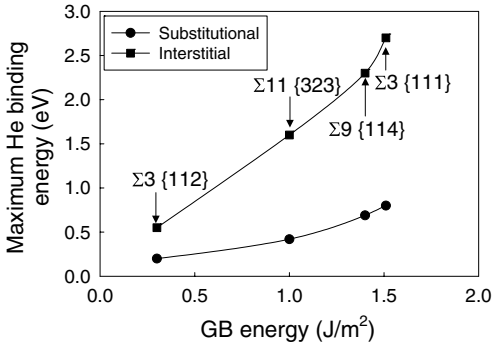

Fig. 2. Maximum binding energy of both interstitial and substitutional He atoms on GBs as a function of GB energy.

4. Diffusion of He interstitial in Σ3{1 1 2} and Σ11{3 2 3} GBs

The lowest energy configurations of a single He atom at the GBs were determined by the procedure described in the previous section. The most stable configuration of a He interstitial in the Σ3 GB is a ⟨$\bar{1}$11⟩ crowdion defect with Fe atoms, while in the Σ11 GB a tetrahedral He interstitial is the most

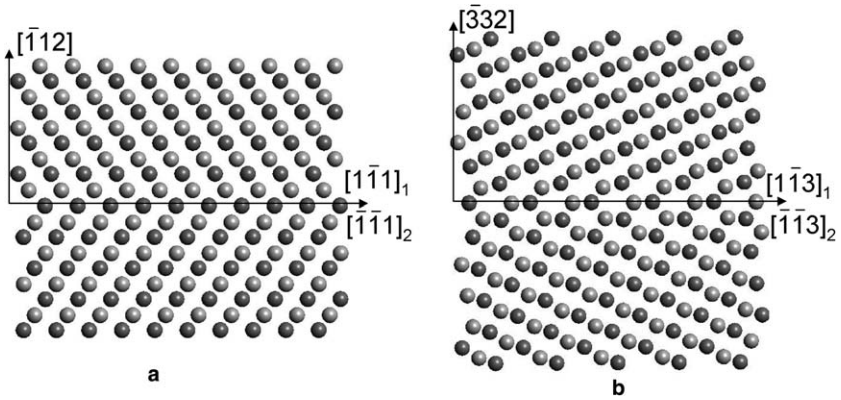

Fig. 1. Relaxed ground state atomic structures for GBs in α-Fe (a) $\Sigma3\langle110\rangle\{112\}$ and (b) $\Sigma11\langle110\rangle\{323\}$, where dark and light spheres represent atom positions in alternating {101} planes perpendicular to the ⟨101⟩ tilt axis.

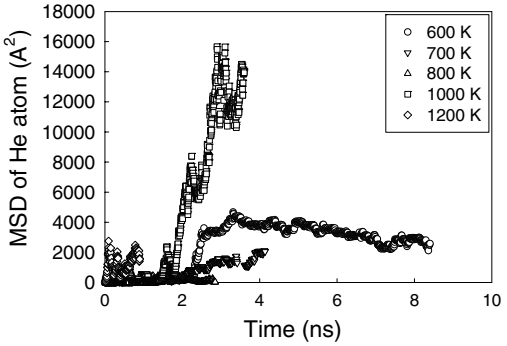

Fig. 3. Mean-square displacements (MSDs) of the He atom as a function of time for the temperature range between 600 and 1200 K on Σ3 GB.

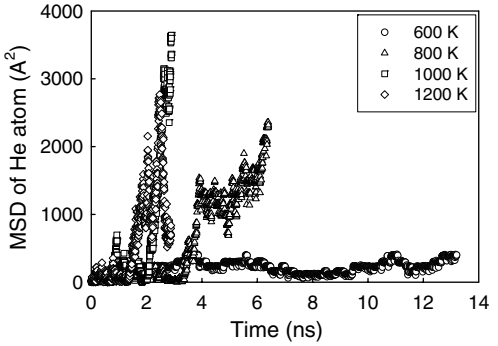

Fig. 4. Mean-square displacements (MSDs) of the He atom as a function of time for the temperature range between 600 and 1200 K on Σ11 GB.

stable configuration. These stable configurations are used as the initial starting configurations for investigating the migration of He interstitials in the temperature range of from 600 to 1200 K. For the Σ3 GB the mean square displacements of the He interstitial are plotted as a function of time in Fig. 3. All the MSDs increase with increasing time, and are approximately linear with time. However, there exist some large fluctuations in the MSD, which may lead to large errors in the estimation of activation energy for He diffusion. As described above, the trajectory of the He atom has been divided into N segments of equal time interval, and the number of segments is varied from 10 to 500 ps. For simulation time up to several tenth ns, the diffusion coefficient can be estimated with a high accuracy. It should be noted that in our MD approach the velocities of atoms are initially scaled to the required temperature with a Gaussian distribution of kinetic energy, and this may lead the He interstitial to a high-energy configuration. Consequently, the MD block is equilibrated for 50 ps before recording the MSD of atoms or He interstitial, which guarantees that the local heat of the interstitial disperses into the surround material. During the simulation, a large number of He jumps are observed, but the dynamic processes occasionally involve the jumps of Fe atoms. However, the contribution of Fe jumps to the total MSD is negligible. The MSDs of the He interstitials simulated in the Σ11{323} GB are shown in Fig. 4. In general, the trend of the MSD is similar to that observed in Σ3 GB, but the MSD values are somewhat smaller. This may be associated with the atomic structures of the GBs, and the migration mechanisms of the He interstitial that will be discussed later. The diffusion coefficients estimated for the He interstitial in both GBs are given in Fig. 5 as a function of reciprocal temperature, where circle symbols represent the data calculated for the Σ3 GB and square symbols indicate the data obtained for the Σ11 GB. The data approximately follow an Arrhenius relationship (Eq. (2)), from which the corresponding activation energies, E_m, and pre-exponential factors, D_0, can be determined. The best fits of these results to Eq. (2) give the values of E_m and D_0 to be 0.28 eV and 4.39×10^{-4} cm^2/s for the Σ3 GB, and 0.34 eV and 4.3×10^{-4} cm^2/s for the Σ11 GB, respectively. It should be noted that the data at 1200 K in the Σ3 GB is excluded for the evaluation of activation energy because the He interstitial dissociates from the GB at this temperature, migrating three-dimensionally. This is consistent with the small binding energy of a He interstitial to the Σ3 grain boundary. The migration energies of He interstitials in GBs are higher than that of a He interstitial in the bulk

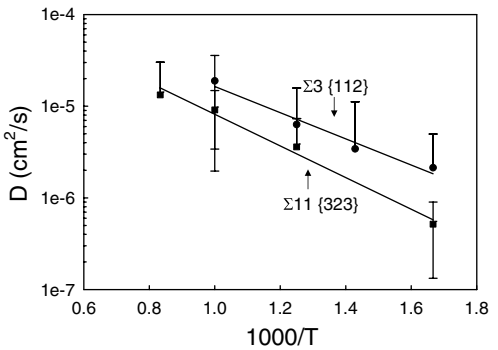

Fig. 5. Diffusion coefficients of He interstitial as a function of reciprocal temperature in Σ3 and Σ11 GBs in α-Fe, where reciprocal temperature is scaled by 1000.

(0.08 eV). In bulk Fe, He interstitials have very high mobility, and they can migrate from one octahedral site to another before being trapped at a dislocation or a GB or becoming deeply trapped in a radiation-induced or thermal vacancy as substitutional helium. The migration trajectory of a He interstitial in the bulk shows that it migrates three-dimensionally. The strong binding of He interstitials to the GB, as shown in Fig. 2, may exhibit its three-dimensional random walk, which possibly gives rise to the higher activation energies in the GBs. However, the activation energies obtained in the present work suggest that He interstitials are very mobile in the GBs, and grain boundaries provide fast diffusion paths for He interstitials along some specific directions.

5. Diffusion mechanisms of He interstitial in GBs

The migration mechanisms of He interstitials in GBs have been studied by carefully analysis of the computer-generated trajectories. The trajectories of the He interstitial in the $\Sigma 3$ GB are shown in Fig. 6(a) for the temperature of 600 K, where gray spheres represent Fe atoms in three $(1\,1\,0)$ atomic planes. The middle plane is the plane containing the initial starting site of the He interstitial. At 600 K, the He interstitial mainly migrates along a $\langle 1\,1\,0\rangle$ direction that is parallel to the tilt axis, but some displacements are observed along the $\langle 1\,\bar{1}\,1\rangle$ direction. This can be further demonstrated by plotting the components of the MSD along $\langle 1\,1\,0\rangle$, $\langle 1\,\bar{1}\,1\rangle$ and $\langle \bar{1}\,1\,2\rangle$ directions as a function of time, as shown in Fig. 6(b). Although there are some fluctuations of the MSD along $\langle 1\,\bar{1}\,1\rangle$ and $\langle \bar{1}\,1\,2\rangle$ directions, the large increase in the MSD is due to the contribution of the $\langle 1\,1\,0\rangle$ component. These results suggest that the He interstitial mainly migrates with one-dimensional behavior at low temperature. However, the migration path of the He interstitial changes from one-dimensional (1D) diffusion to two-dimensional (2D) diffusion with increasing temperature. The trajectories of the He interstitial at 800 K are shown in Fig. 7(a), while the MSDs along each direction are plotted as a function of time in Fig. 7(b). The two-dimensional migration behavior of the He interstitial is obviously observed in the trajectories of the He interstitial, which is consistent with the MSDs along different directions. The MSDs along both the $\langle 1\,1\,0\rangle$ and $\langle 1\,\bar{1}\,1\rangle$ directions show large variations with increasing time, but there is little variation along the $\langle \bar{1}\,1\,2\rangle$ direction. The further increase in temperature (up to 1200 K) leads to the dissociation of the He interstitial from the $\Sigma 3$ GB, in consistent with its small binding energy, which is the lowest He binding energy among all the GBs calculated, as shown in Fig. 2. The dissociation allows the He interstitial to also migrate along $\langle \bar{1}\,1\,2\rangle$ direction, resulting in three-dimensional (3D) diffusion. This change in migration process from 1D to 3D makes it difficult to accurately calculate the activation energy of the He interstitial since the migration mechanism itself has a pronounced dependence on the temperature. Actually, it is important to point out that the activation energy obtained for the $\Sigma 3$ GB is an effective activation energy. The temperature dependence of the MSD regarding diffusion along different directions sug-

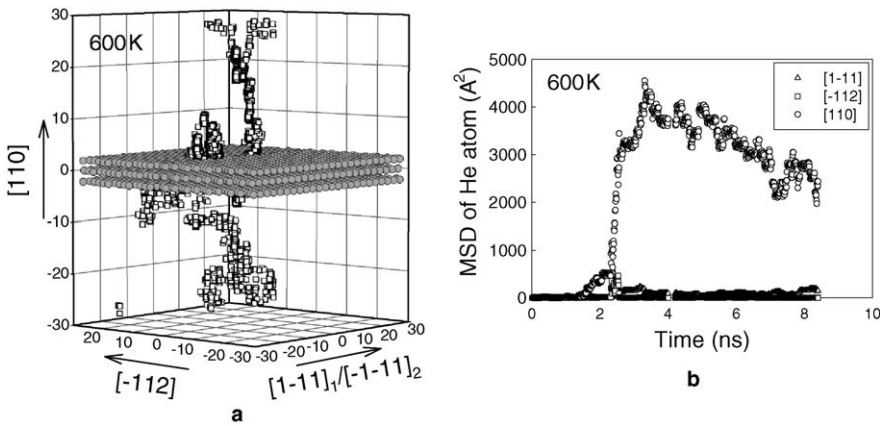

Fig. 6. (a) Trajectories of He interstitial at 600 K in $\Sigma 3$ GB, where three $(1\,1\,0)$ atomic planes are presented, as indicted by light spheres, and (b) MSD of He interstitial along $\langle 1\,\bar{1}\,1\rangle$, $\langle \bar{1}\,1\,2\rangle$ and $\langle 1\,1\,0\rangle$ directions at the same temperature.

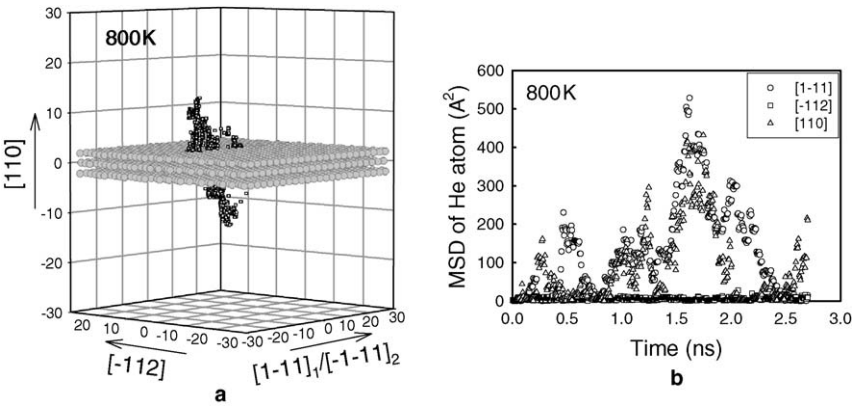

Fig. 7. (a) Trajectories of He interstitial at 800 K in Σ3 GB, where three (1 1 0) atomic planes are presented, as indicted by light spheres, and (b) MSD of He interstitial along $\langle 1\,\bar{1}\,1\rangle$, $\langle \bar{1}\,1\,2\rangle$ and $\langle 1\,1\,0\rangle$ directions at the same temperature.

gests that the migration barrier along the $\langle 1\,1\,0\rangle$ direction should be lower than that along the $\langle \bar{1}\,1\,2\rangle$ direction. Future work using the dimer method [21] should provide more fundamental understanding of different mechanisms involved in the diffusion processes of He interstitials, particularly at extended defects such as dislocations and grain boundaries.

The trajectories of the He interstitial and the MSDs along three independent directions in the Σ11 GB at 1000 K are shown in Fig. 8(a) and (b), respectively. Similar to the plots in Figs. 6 and 7, only three atomic planes normal to the tilt axis are presented in Fig. 8(a). Although the He interstitial can move in the spaces between the three planes, it is strongly bound to the middle plane on which the initial starting position of the He interstitial is allocated. It is of interest to note that the He interstitial migrates one-dimensionally along the $\langle 1\,\bar{1}\,3\rangle$ direction, even at higher temperatures. Also, the MSD plots in Fig. 8(b) indicate that the He interstitial migrates only along the $\langle 1\,\bar{1}\,3\rangle$ direction. Although only two GBs have been considered in these diffusion simulations, the results demonstrate that interstitial He diffusion and the corresponding migration mechanisms depend significantly on the atomic structures of the GBs. If a He interstitial is strongly bound to a GB, it is more likely that one-dimensional migration of the He interstitial along the GB direction is a dominant mechanism. It is worth pointing out that the variation in diffusion mechanisms of He interstitials in GBs should have significant effects on He bubble nucleation at different GBs.

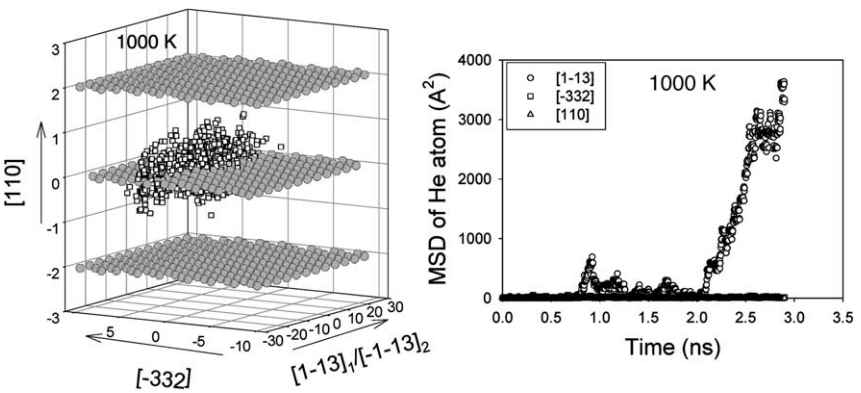

Fig. 8. (a) Trajectories of He interstitial at 1000 K in Σ11 GB, where three (1 1 0) atomic planes are presented, as indicted by light spheres, and (b) MSD of He interstitial along $\langle 1\,\bar{1}\,3\rangle$, $\langle \bar{3}\,3\,2\rangle$ and $\langle 1\,1\,0\rangle$ directions at the same temperature.

6. Summary

Helium diffusion along the GBs in α-Fe has been studied using molecular dynamics methods, and two grain boundaries, $\Sigma11\langle110\rangle\{323\}$ and $\Sigma3\langle110\rangle\{112\}$, were used for the current investigations. The effect of GB structure on the binding energy of He is firstly explored to characterize He properties in different GBs. Results of static relaxations reveal that both substitutional and interstitial He atoms are bound to all the GBs studied, with interstitial He being more strongly bound to the GB core than substitutional He. The binding energies of He atoms are found to increase with increasing GB energy, which is also related to the increasing excess volume in the GB.

Migrations of He atoms were followed for 1–14 ns, at temperatures between 600 and 1200 K. The diffusion coefficient of He atoms is calculated using the mean square displacements of He atoms, and the effective migration energies were determined to be 0.34 and 0.28 eV for $\Sigma11\langle110\rangle\{323\}$ and $\Sigma3\langle110\rangle\{112\}$ GBs, respectively. He interstitials diffuse rapidly in the $\Sigma11$ GB with one-dimensional migration along the [1–13] direction in the GB. In the $\Sigma3$ GB He interstitials migrate one-dimensionally at low temperature, two-dimensionally at intermediate temperature and three-dimensionally at higher temperature. Three-dimensional diffusion behavior of He interstitial in the $\Sigma3$ GB is an indication of the dissociation of the He interstitial from the GB at high temperatures. The activation energies and diffusion mechanisms of interstitial He are strongly correlated to the binding properties of He atoms to the GB. The different activation energies, He binding energies and He diffusion mechanisms in these two representative grain boundaries suggest that the varying atomic structures of the grain boundaries, especially with respect to excess volume in the GB, are important for the diffusivity of He.

Acknowledgement

This research is supported by the US Department of Fusion Energy Sciences under Contract DE-AC06-76RLO 1830.

References

[1] E.E. Bloom, J. Nucl. Mater. 258–263 (1998) 7.
[2] H. Ullmaier, Nucl. Fus. 24 (1984) 1039.
[3] K. Farrell, P.J. Maziasz, E.H. Lee, L.K. Mansure, in: H. Ullmaier (Ed.), Fundamental Aspect of Helium in Metals, Radiat. Eff. 78 (1983) 1.
[4] S.J. Zinkle, N.M. Ghoniem, Fus. Eng. Des. 51&52 (2000) 55.
[5] R.L. Klueh, D.J. Alexander, J. Nucl. Mater. 218 (1995) 151.
[6] M.I. Baskes, MRS Bull. (1986) 14.
[7] A. Ryazanove, R.E. Voskoboinikov, H. Trinkaus, J. Nucl. Mater. 233–237 (1996) 1085.
[8] H. Trinkaus, B.N. Singh, J. Nucl. Mater. 323 (2003) 229.
[9] Yu.N. Osetsky, D.J. Bacon, A. Serra, B.N. Singh, S.I. Golubov, Philos. Mag. 83 (2003) 61.
[10] B.D. Wirth, G.R. Odette, D. Maroudas, G.E. Lucas, J. Nucl. Mater. 276 (2000) 33.
[11] K. Morishita, R. Sugano, B.D. Wirth, T. Diaz de la Rubia, Nucl. Instrum. and Meth. B 202 (2003) 76.
[12] B.D. Wirth, E.M. Bringa, Phys. Scr. T 108 (2004) 80.
[13] R.J. Kurtz, H.L. Heinisch, J. Nucl. Mater. 329–333 (2004) 1199.
[14] M.I. Baskes, V. Vitek, Met. Trans. A 16 (1985) 1625.
[15] P.A. Thorsen, J.B. Bilde-Sörensen, B.N. Singh, Mater. Sci. Forum 207–209 (1996) 445.
[16] R.J. Kurtz, R.G. Hoagland, J.P. Hirth, Philos. Mag. A 79 (1999) 665.
[17] R.J. Kurtz, R.G. Hoagland, J.P. Hirth, Philos. Mag. A 79 (1999) 683.
[18] G.J. Ackland, D.J. Bacon, A.F. Calder, T. Harry, Philos. Mag. A 75 (1997) 713.
[19] W.D. Wilson, R.D. Johnson, Rare Gases in Metals, in: P.C. Gehlen, J.R. Beeler Jr., R.I. Jaffee (Eds.), Interatomic Potentials and Simulation of Lattice Defects, Plenum, 1972, p. 375.
[20] D.E. Beck, Mol. Phys. 14 (1968) 311.
[21] F. Gao, H.L. Heinisch, R.J. Kurtz, Yu.N. Osetsky, R.G. Hoagland, Philos. Mag. 85 (2005) 619.